

Non-crystalline SiO₂: processing induced pre-existing defects associated with vacated O-atom intrinsic bonding sites

G. LUCOVSKY*, J. W. KIM, K. WU, D. ZELLER, B. PAPAS, J. L. WHITTEN
North Carolina State University Raleigh, N.C., 27695-8202, USA

Electron spin resonance (ESR) studies by Galeener and co-workers on bulk-quenched silica (SiO₂) have distinguished between pre-existing, and X-ray and γ -ray radiation induced defects. Pre-existing defect densities increase exponentially with increasing quenching and annealing temperatures and in “dry silicas” these are assigned to X-ray activated E' centers, singly occupied Si atom dangling bonds. Non-bonding O hole centers, NBOHC defects are also detected in dry silicas, but only after X-ray or γ -ray irradiation, and these defects increase linearly with the radiation dosage. Pre-existing defects have also been detected by 2nd derivative O K pre-edge X-ray absorption spectroscopy in remote plasma deposited and thermally grown SiO₂ and GeO₂ thin films. These spectra display singlet and triplet features labeled according to Tanabe-Sugano diagrams. It is demonstrated by ab initio theory and experiment that pre-existing defects in thin film SiO₂ and GeO₂ are vacated O-atom sites in which an O atom has never resided, rather than O-vacancy sites from which an O-atom bond has been broken and remains within the material. As such Tanabe-Sugano diagram symmetries and singlet and triplet labeling have been extended to d-states on nearest-neighbor Si and Ge dangling bonds in these vacated sites. Vacating O-atoms complement chemical bonding self-organizations that result in medium range order (MRO) as an additional mechanism providing local strain relief. Based on ESR, pre-existing defects (i) in As_{1-x}S(Se)_x alloys, including As₂S(Se)₃, and (ii) in S(Se)-rich Ge_{1-x}S(Se)_x alloys are qualitatively different that pre-existing defects in (i) SiO₂ and GeO₂, and (ii) GeS(Se)₂. These differences are associated with fundamental differences in their respective electronic structures.

(Received November 1, 2011; accepted November 23, 2011)

Keywords: SiO₂, Defects, Oxygen sites

1. Introduction

Before explaining differences in ESR active pre-existing defects in SiO₂ and As_{1-x}S(Se)_x alloys, it is necessary to discuss qualitative differences in medium range order (MRO) in these markedly different non-crystalline materials. This is addressed in the context of electronic spectroscopy and theory based on d-state ligand field splittings associated with molecular orbital theory descriptions of valence band states.¹⁾ The ligand field splitting, $\Delta\text{LF}(\text{Xi})$, in eV at a Si, Ge and As cation site, Xi, in oxides and chalcogenides has been obtained from analysis of X-ray absorption and electron energy loss spectroscopies, and also from the imaginary part of the complex dielectric, ϵ_2 , from reflectivity (R), and spectroscopic ellipsometry (SE) spectra. $\Delta\text{LF}(\text{Xi})$ is local symmetry, atomic coordination, and atom specific. A non-vanishing value requires a scale of coherent order extending to up to, and generally beyond, 3rd next-nearest-neighbors into a medium range order (MRO) regime including discrete values of dihedral angles.¹⁾ As such, a non-vanishing ΔLF is a spectroscopic indicator for MRO, complementing traditional X-ray and neutron diffraction approaches based on the position and width of the first sharp diffraction peak (FSDP).²⁾ This approach provides a connection with the detection of pre-existing ESR active

defects in SiO₂, and differences between pre-existing ESR active defects in SiO₂ and GeO₂, and As_{1-x}Se_x and Ge_{1-x}Se_x chalcogenide alloys, including compound compositions such as As₂S(Se)₃ and Ge₅(Se)₂.

MRO regime atomic correlations have been obtained experimentally from the position FSDP in the structure factor from X-ray or neutron diffraction.²⁾ Inter-atom correlation lengths, λ_{corr} , are 0.4 nm in SiO₂,⁴⁾ and extend to ~0.65 nm in GeSe₂.^{2,3)} A coherence length, λ_{coh} , for cluster formation is obtained from the FSDP width is beyond the MRO regime, e.g., λ_{coh} is ~1 nm in Si(Ge)O₂,³⁾ 2.1 nm in GeSe₄, and 2.9 nm in GeSe₂.⁴⁾ Ab-initio calculations on terminated small clusters demonstrate that λ_{corr} in non-crystalline SiO₂, silica, and crystalline SiO₂ is derived from the *back-donation* of electrons from occupied O 2p π non-bonding orbitals into empty Si atom 3d orbitals, and is facilitated by of the large Si-O-Si bond angle of ~150°. ⁵⁾ In non-crystalline chalcogenides, bonding correlations beyond nearest neighbor bond-lengths and bond-angles derive from a minimization of *repulsions between non-bonding p π states* on S, Se, and As. ⁶⁾ This results from smaller S- and Se-centered bond chalcogenide non-crystalline thin films/glasses annealed at the glass transition temperature in compounds including As₂S(Se,O)₃, GeS(Se)₂ and Si(Ge)O₂ and binary As_{1-x}Se_x and Ge_{1-x}Se_x alloys. These

materials are not CRN's because they have MRO. In contrast, Since $\Delta LF = 0.0$ for a-Si (Ge), and a-III-V's with no dihedral angle ordering, or third next N-N XRD features, these are *bona-fide* CRN's as defined by SRO bond-lengths and bond-angles.⁷ These differences establish a significant role for spectroscopic ΔLF determination as a complementary and reliable probe beyond X-ray and neutron diffraction as an indicator for MRO.

2. Pre-existed defects in SiO₂: O K pre-edge spectra

Ab initio theory and experiments indicate that (i) pre-existing defects in thin film SiO₂ are vacated O-atom sites, rather than bona-fide O-vacancies from which an O-atom has been displaced by bond-breaking, but remains within the network. A relationship between pre-existing defects in SiO₂ and medium range order (MRO) results from discrete dihedral angles extending to third and sometimes fourth nearest-neighbors (NN's).⁸ This scale of MRO has been established by analysis of the first sharp diffraction peak (FSDP) in the structure factor from X-ray or neutron diffraction of bulk glasses,^{1,3} and subsequently extended to thin films. Analysis of the FSDP yields inter-atomic correlation lengths in SiO₂ of ~ 0.4 to 0.5 nm corresponding to discrete dihedral angles bridging Si-O-Si bonds, and larger coherence lengths defining non-periodically organized clusters with dimensions ~ 1 nm, which include the discrete dihedral angles as determined in Ref 8.

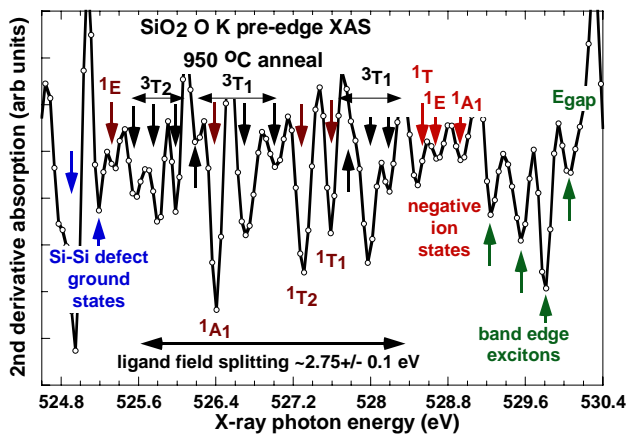


Fig. 1. O K pre-edge 3rd derivative spectrum for remote plasma deposited SiO₂ annealed at 950C for 1 minute in Ar.

Fig. 1 is a high resolution 2nd derivative O K pre-edge X-ray absorption spectra for an SiO₂ film annealed in Ar at 950°C: (i) the band-gap, (ii) 3 band edge excitons, (iii) 3 negative ion singlet states, (iv) inter-connected triplet, and singlet terms, and (v) singlet and triplet ground states. Fermion wave functions are anti-symmetric 4-vectors (see Fig. 2). Labeling of features in Fig. 1 is from

the d^2 Tanabe-Sugano (T-S) diagram for tetrahedrally-bonded Si, and for intermediate values of ΔLF .¹ The T-S diagrams were developed for occupied d-states on single TM-atom, however, the same group theoretically-allowed transitions occur also apply to two occupied d-states on the same nd, e.g., $n = 3$, in close proximity, e.g., up to 0.3 to 0.4 nm. The relative strengths of defect terms and band edge excitons in SiO₂ films display approximately the same temperature dependence as the D₂ Raman peak for films annealed at $\sim 875^\circ$ to 900°C and 950°C .⁹

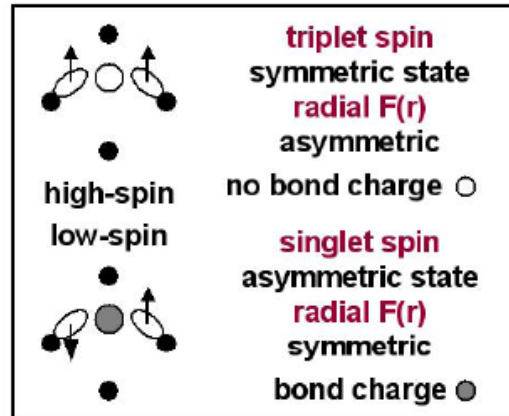


Fig. 2. Schematic representation of the symmetries of the radial spatial and spin contributions to singlet and triplet two electron Fermion wave functions of two electrons in close proximity, ~ 0.25 to 0.45 nm.

Fig. 2 includes the symmetries of the radial spatial and spin contributions to the singlet and triplet two electron Fermion wave functions. The important differences in orbital geometries between process-induced vacated O-bonding sites and O-vacancies created by stress are indicated in Fig. 3. The orbital geometry for the O-vacancy has the same Si-O-Si bond-angle as in SiO₂, 148°C and the Si orbitals are not co-linear as they are for the vacated O-site. When the distance between two Si atoms bordering the vacancy is increased, the 3-fold symmetry is maintained for Si-atoms back-bonded to the network. The Raman and IR frequencies for 4-symmetric Si-O bonds are 800 cm^{-1} ;⁹ scaled to 3-symmetric Si-O bonds this yields a frequency of $\sim 600\text{ cm}^{-1}$, providing a new assignment for the Raman D₂ feature.¹⁰ The results of ab initio calculations based on two electron wave functions for the two geometries in Fig. 3 are included in Fig. 4, which includes the variation of the single and triplet ground state energies as function of the distance between the Si atoms. As expected, both the exchange energy and the radial wave function, $F(r)$ overlap are larger for the vacated site. For Si-Si distances $> 3.6\text{ \AA}$, the dependence of ground state energies is the same for both orbital geometries. The DFT studies of the Robertson and Shlugger groups indicate that TM atoms bordering a vacancy show relatively small relaxations of order 0.1 - 0.2 \AA , and as such the only possible ground state and excited states in DFT studies have a singlet character.^{11,12}

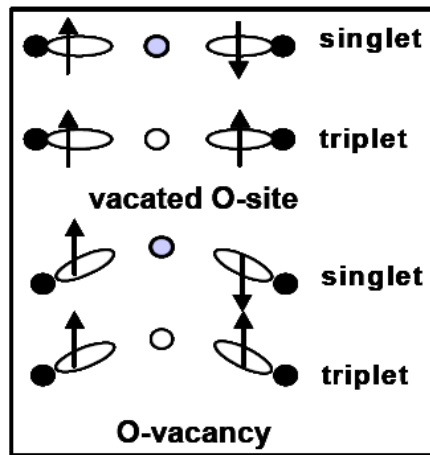


Fig. 3. Schematic representation of important differences in orbital geometries between process-induced vacated O-bonding sites, and O-vacancies created by X-ray or γ -ray radiation resulting in ejection of a neutral O-atom.

The results in Fig. 4 explain the fundamental differences and similarities between ab initio calculations and the DFT results. First, the only possible ground states in DFT calculations are singlet states, so that they cannot explain all of the spectroscopic studies of the Lucovsky group which yield both singlet and triplet features in the O K pre-edge spectra of TM oxides,¹³ and SiO₂ and GeO₂ as well. In addition, the energies of the singlet ground states calculated by the Robertson group are generally >3 eV above the valence band edge. The energy separation between these states and negatively charged O-vacancies is significantly smaller than what has been reported by the Lucovsky group, because DFT calculations are not based on molecular orbital ground states that inherently include d-state Δ LF splittings.¹

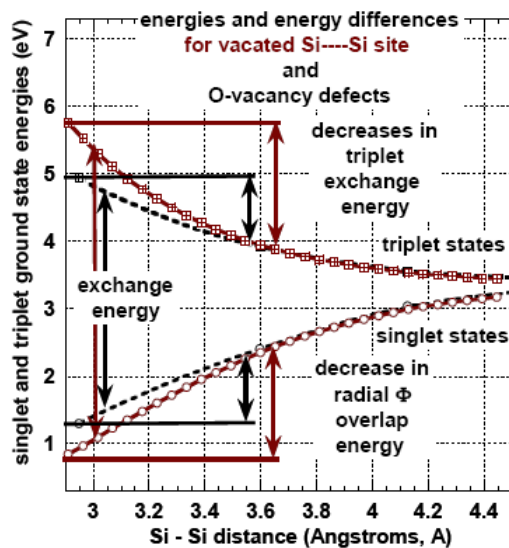


Fig. 4. Plot of the variation of the single and triplet ground state energies as function of the distance between the Si atoms for a vacated O-atom site, and an O-vacancy created by X-ray or γ -ray radiation resulting in ejection of a neutral O-atom.

In contrast, ab initio quantum chemistry calculations yield both singlet and triplet features for pre-existing defects in TM oxides and SiO₂ consistent with Fig. 4 and T-S diagrams.^{1,5} As noted above, preliminary measurements on SiO₂ films as-deposited and annealed at different temperatures establish (i) as-deposited films display both singlet and triplet features, and (ii) singlet features increase in strength as annealing temperatures are increased consistent with the new proposed interpretation for D₂.

3.ESR - active defects in SiO₂

ESR features in SiO₂ films exposed to X-rays, γ -rays and high energy electrons have been interpreted with an O-vacancy mechanism in which electrons are in doubly-occupied dangling bond states.¹⁴ The ESR E' center is a singly occupied dangling bond attached to three-fold Si, requiring activation by high-energy electrons, X-rays or γ -rays. Since O-atoms do not form O-O pair bonds other than peroxy-radicals, they are easily not accommodated in SiO₂ networks, but instead give rise to non-bonding O-associated hole center (NBOHC) defects in irradiated films or glasses.^{10,14} These centers are formed by breaking one of the two Si-O bonding of the bridging Si-O-Si bonding arrangement in SiO₂ networks.

Electron spin resonance (ESR) studies by Galeener and co-workers on bulk-quenched silica (SiO₂) have distinguished between pre-existing, and X-ray and γ -ray radiation induced defects.¹⁰ Pre-existing defect densities increase exponentially with increasing quenching and annealing temperatures and in “dry silicas” these are assigned to E' centers which are singly occupied Si-atom dangling bonds. NBOHC defects are also detected in dry silicas, but only after X-ray or γ -ray irradiation, and these defects increase in number linearly with increasing radiation dosage. Pre-existing defects have also been detected by 2nd derivative O K pre-edge X-ray absorption spectroscopy in remote plasma deposited and thermally grown SiO₂ and GeO₂ thin films.

It is important to differentiate between (i) pre-existing and (ii) radiation, and electron and neutron induced defects in “wet” and “dry” silica,^{10,14} since this differentiation is also important in understanding differences in ESR defects in GeS(Se)₂ and As₂S(Se)₃. The “dry-silica” results correspond directly with pre-existing defects in plasma-deposited and annealed thin films of GeO₂ and SiO₂, and GeS₂ as well, whereas, ESR defects in S-rich Ge_{1-x}S_x,¹⁵ and As₂(S,Se)₃.^{16,17} are similar to “wet-silica” results. The pre-existing “wet silica” defects are NBOHC's indicating qualitatively different defects when compared with pre-existing defects in “dry silicas”. In each instance these require activation, for example optical or UV radiation, for ESR detection.

Returning to “dry-silica” glasses, plots of ESR line strength versus X-ray exposure time for E' center defects for glasses quenched from two different fictive temperatures, 1000°C and 1350°C is presented in Fig. 1 of Ref 10. The x = 0 intercepts are in agreement with the

assignment of pre-existing features as E' centers. There are no pre-existing non-bridging O-hole center (NBODC) defects in "dry-silica", consistent with pre-existing vacated O-atom site description. Glasses irradiated by X-rays and γ -rays, and high energy electrons and neutrons indicate increased numbers of E' centers as shown in Fig. 1, as well as NBODC and peroxy-radical defect centers.^{fig1985)}

Galeener and co-workers have proposed that two features in the Raman spectrum of pristine SiO₂ are associated with small regular rings of bonded atoms.³⁾ They labeled these as D₁ and D₂; however, when they discussed pre-existing ESR-active defects, they suggested that D₁ and D₂ were not necessarily related to these defects. This is inconsistent since there are clearly pre-existing ESR-active defects in "dry silicas" which display shows a significant increase the ESR signal for pre-existing defects, increasing by a factor of about 2 for annealing at 1000°C and 1350°C in Fig. 1, approximately the same as the increase in D₂.

Equally important, the assignments of Galeener are not consistent with spectroscopic studies of remote plasma deposited and annealed SiO₂ and GeO₂. These studies have identified O K pre-edge sub-band gap features that are assigned to vacated or empty O-atom sites, i.e., pre-existing defects, as distinguished from O-vacancies produced by irradiation. Moreover, as already noted above, the 800 cm⁻¹ IR/Raman frequency symmetric bond-stretching mode provides a way to estimate the frequency of D₂ defect feature addressed above.⁹⁾ The 800 cm⁻¹ is a symmetric stretching of four Si-O bonds. For the vacated O-atom site discussed above the defect is a singly occupied neutral Si dangling bond back-bonded to three O-atom nearest neighbors in geometry that has three-fold symmetry. This bonding arrangement has a symmetric IR and Raman active mode, indicating that the D₂ defect is associated with a symmetric stretching of three Si-O bonds, rather than an O-breathing mode in a small ring structure.¹⁰⁾ To first order, this assignment this predicts a D₂ vibrational frequency three-quarters of 75% of the symmetric stretch for the IR/Raman 800 cm⁻¹, or ~600 cm⁻¹, in excellent agreement with position of the D₂ frequency in Raman spectra.

4. ESR - active defects in chalcogenides

Similar to plasma-deposited SiO₂ and GeO₂, the stoichiometric GeS₂ compositions contain small concentrations of detectable pre-existing ESR defects.¹⁸⁾ However, for Ge concentrations between about 20 at. % and about 31.5 at. %, two defect signatures are evident, one characteristic of an E' center on the Ge atoms, and the second a non-bridging S-atom hole center (NBSHC) center on the S atoms. These conjugate defects result from local strain induced breaking a Ge-S bond, into a Ge dangling bond back-bonded to the three S-atoms of the network, and a terminal and neutral singly occupied S dangling bond. Paired pre-existing defects of this sort have not been reported in non-crystalline S-rich concentrations As_{1-x}(S,Se)_x alloys, or in SiO₂ and GeO₂ thin films. Local strain in SiO₂ and GeO₂ is relieved by vacating bridging

O-atoms, whereas the lower average coordination in chalcogenide rich As-S and As-Se alloys is insufficient to force defect formation by vacating or bond breaking mechanisms, and as such there are not reports of pre-existing defects in these alloys, or in stoichiometric compounds as well.

Complementary studies of amorphous As and Se, and As₂Se₃ were performed by the NRL group of Bishop, Taylor and Strom.^{16,17)} These studies performed at low temperatures, demonstrated an optically induced ESR signal in As₂Se₃ by excitation in the Urbach tail, absorption constant ~100 cm⁻¹, and accompanied by mid-band gap absorption. The NRL group has attributed the ESR response in As₂S₃ and As₂Se₃, respectively, to a single electron occupancy in non-bonding S 2p π and Se 3p π lone pair orbitals, that is to NBS(Se)HC's. The ESR "dry-silica" glasses spectral functions are qualitatively similar to the NBOHC ESR in SiO₂. Finally, the Xerox PARC group of Biegelsen and Street demonstrated qualitatively different ESR signals for optically induced ESR in As₂Se₃ in the Urbach tail, and at higher photon energy as which photo-darkening occurred,¹⁹⁾ confirming significant SRO and MRO scale bonding changes in the photo-darkened state. These local changes in SRO and MRO have identified in EXAFS studies, PS) and ab-initio calculations.

6. Summary

(i) Quantification of MRO has been achieved by analysis of the FSDP in the structure factor obtained from analysis of X-ray and neutron ^{2,3)} This extends to 3rd and 4th NN's and as such includes discrete values of dihedral angles, and in many instances coupled phase relationships between these discrete dihedral angles.⁸⁾

(ii) MRO has also been detected by d-state ligand field splittings, ΔLF 's, that derive from the valence band states comprised of symmetry-adapted linear combinations (SALC's) of atomic states.¹⁾ These splittings are evident in Si and L_{2,3} and Ge M_{2,3} spectra, respectively, for SiO₂ and GeO₂, UPS and XPS valence band spectra, conduction band spectra obtained by spectroscopic ellipsometry and reflectivity, as well as O K edge XAS spectra.

(iii) ΔLF 's and hence MRO can also be obtained from analysis of O K pre-edge defect spectra. This approach treats the two electrons localized at an O-vacancy, or in a vacated O-atom site as a strongly-correlated pair on two different atoms, and then applies T-S diagrams as the basis for extracting values of ΔLF .¹³⁾

(iv) Proceeding in this the vacated O-atom site model has been verified by a combination of ab-initio quantum chemistry calculations and the O K pre-edge spectra for SiO₂, and GeO₂.

(v) The vacated O-atom site model has been extended to a vacated S (Se)-atom model for GeS(Se)₂. Due to catenation of S- and Se-atoms in S(Se)-rich Ge_{1-x}S(Se)_x and in all As_{1-x}S(Se)_x alloys, the vacated S(Se)-atom site models do not apply.

Finally, (vi) it is significant to note that pre-existing defects in SiO₂ and GeO₂ are thermally-activated by removal from Si-O-Si and Ge-O-Ge bonding sites within the chemically self-organized clusters geometries extracted from the analysis of the FSDP. In a similar way, the limiting defect densities in a-Si(H) with 10 at.% H are associated with thermal activation of Si-H vibrations at the perimeter of the self-organized clusters in a-Si(H) alloys.

Acknowledgements

The authors acknowledge support from the AFOSR and DTRA. The unique character of Beam Line facilities at SSRL in Menlo Park, CA is gratefully acknowledged. Most importantly this paper was finalized on the last day of my dear wife's life, September 10, 2011. She was the "love of my life" and her tenderness and constant support always shown through. She lives in my heart forever, and this paper, along with another one in these proceedings is a testimony to her courage that has continued to sustain me.

References

- [1] F.A. Cotton, Chemical Applications of Group Theory, 2nd Ed. (Wiley Interscience, New York, 1963) Chapter 8.
- [2] J. Du, R.L Corrales, Phys. Rev. B **72**, 092201 (2005).
- [3] S.C. Moss and D.L. Price: in Physics of Disordered Materials, edited B. D. Adler and H. Fritzsche S.R. Ovshinsky (Plenum Press, New York, 1985), p. 77; D.L. Price et al., J. Phys. Condens. Matter **1**, 1005 (1989).
- [4] N.R. Rao, et al., J. Non-Cryst. Solids **240**, 221 (1998).
- [5] J. L. Whitten, et al., J. Vac. Sci. Technol. B **20**, 1710 (2002).
- [6] G. Lucovsky, J.C. Phillips, J. Phys.: Condens. Mater. **19**, 455218 (2007).
- [7] B. Kramer, K. Maschke and P. Thomas, phys. stat. sol. (b) **49**, 525 (1972).
- [8] G. Lucovsky, F.L. Galeener, J. of Non-Cryst. Solids **35 & 36**, 1209 (1980).
- [9] F.L. Galeener and G. Lucovsky, Phys. Rev. Lett. **37**, 1474 (1976).
- [10] F.L. Galeener, J. Non-Cryst. Solids **71**, 373 (1985); Phys. Rev. B **47**, 7760 (1993).
- [11] K. Xiong, et al., Appl. Phys. Lett. **87**, 183505 (2005).
- [12] L. Gavartin, et al., Appl. Phys. Lett. **89**, 082908 (2006).
- [13] G. Lucovsky, Japan J. Appl. Phys. **50**, 04DC09 (2011).
- [14] D.L. Griscom, Ceramic Soc. Jap. **90**, 823 (1981), and Refs. therein.
- [15] K. Arai and H Namikawa, Solid State Commun. **13**, 1167 (1973).
- [16] S.G. Bishop et al., Phys. Rev. Lett. **21**, 1346 (1975)
- [17] S.G. Bishop et al., Phys. Rev. B **15**, 2294 (1977).
- [18] R.A. Street, D.J. Biegelsen, J. of Non-Cryst. Solids **32**, 339 (1979).
- [19] D.K. Biegelsen and R.A. Street, Phys. Rev. Lett. **44**, 803 (1980).
- [20] G. Lucovsky, et al., Paper ID. 1350 of these proceedings.
- [21] G. Lucovsky, et al. Paper ID 1312 of these proceedings.

*Corresponding author: lucovsky@ncsu.edu